

ADAPTIVE SCANNING OF DIVERSE HERITAGE ORIGINALS LIKE SYNAGOGUE INTERIOR, EMPTY RARE PAPERS OR HERBARIUM ITEMS FROM THE 19th CENTURY

**BOHDAL Róbert (SK), BÁTOROVÁ Martina (SK), FERKO Andrej (SK),
FABIÁN Marián (SK), HRABOVSKÝ Michal (SK), LÚČAN Ľubomír (SK),
ZABADAL Ľubomír (SK)**

Abstract. We create the digital twins using the hi-tech CRUSE CS 220ST1100 contactless scanner, providing high precision both in geometry and radiometry. We survey many sharpness functions and we report results of experiments examining how to manually focus the scanner, applying the Fourier transform. We have created the exact representation of interior of a non-existing building, and we also wanted to achieve as true colors as possible of a collection of rare blank handmade papers. Further, we have analyzed requirements for documenting Herbarium data. We discuss selected uncertainty and educational issues within this context.

Keywords: digitization, Fourier transform, 3D modeling, virtual reality

Mathematics Subject Classification: 68U05, 68U07.

1 Introduction

Virtualization of cultural or natural heritage has become an important part of the knowledge economy in EU. We create the digital twins using the hi-tech CRUSE CS 220ST1100 contactless scanner, providing high precision both in geometry and radiometry. We report on manual focusing, two case studies in progress and specify another one. We review relevant previous work, in part 2. Part 3 reports on survey of 21 functions and manual focusing experiments. Parts 4 and 5 describe the interior reconstruction and rare papers case studies. We discuss specification issues for herbarium in Part 6, and selected uncertainty and educational issues within this context, in Part 7.

2 Preliminaries and Previous Work

In general, in virtual reality and CAD, we minimize errors in the 8-dimensional $(x, y, z, t, r, g, b, \alpha)$ parameter space. The α parameter expresses the transparency in an interval

[0,1], the (r,g,b) triplet represents color values, t means time and (x,y,z) spatial coordinates in projectively extended Euclidean space. The Cruse Scanner solves the error minimization problem by measurement within a 5-dimensional parametric subspace (x, y, r, g, b) . It is possible to scan the given scanline of real artwork under constant illumination accurately up to 1200 ppi (pixels per inch) in the TIFF format. The scanned original weight may be up to 300 kg, measuring 120×180×30 cm [3, 4]. The current software CSx does not create a 3D model, but allows for precise TIFF scanning with variable illumination, 15-degree sensor rotation and variable depth of field, thus offering dozens of scan versions of a single original. The (r,g,b) color primaries can be stored in 48-bit color depth. We study the accuracy of the scan and the speed of the related processes, in order to optimize for given data type.

Of course, there exist no absolutely exact scanned values, as the top quality CCD “14.400 Pixel Tri Linear RGB Line-Sensor” with Schneider optics has its own limitations. When solving real world problems, we rarely avoid uncertainty [9]. On empirical level, each measurement is burdened by the error of the instruments, and at the cognitive level, the uncertainty can also come from the vagueness and ambiguity of the language used, at the psychological level at uncertainty impinges the individuality of perception, education, experience etc. Despite the uncertainty, we decide and solve problems, often using computers. The three types of uncertainty are vagueness (fuzziness), nonspecificity, controversy (strife). The latter two can be referred to as ambiguity. We have to be aware of approximation, extrapolation, and even of missing data or metadata, while creating real documentation or virtual exhibitions.

The digitization of hundreds of thousands museum originals in Slovakia is reflected e.g. in [8, 11, 12]. Slovak National Gallery seems to offer the best presentation and documentation of visual arts [2], running three similar Cruse scanners on everyday basis. One of the projects was *Comeniana – methods and means of digitization and presentation of 3D objects of cultural heritage*. The team developed and implemented 8 data acquisition modes, including Cruse scanning. The most valuable Comenius University heritage items were scanned in a suitable way, see *Comeniana Showreel* at YouTube [17].

3 Manual Focusing of the Cruse Synchron Table Scanner

The scanner Cruse does not provide the autofocus option. If we want the resulting scanned image to be sharp enough, we need to know the height of the scanned object and rely on the correct adjustment and calibration of the optical system. Since both conditions are not always easy to accomplish, the scanner provides a manual focus feature that utilizes the image sharpness measure based on the Fourier transform.

In CCD-based digital cameras, active or passive focusing systems are used. The active systems emit ultrasound or infrared waves. Based on the time interval when the reflected wave returns to the sensor, they calculate the distance to the scanned object. Passive systems determine sharpness by means of sharpness functions in which a distinct local or global extreme is found.

The sharpness function calculates the sharpness function using the pixel values of the scanned image. The sharpness function value varies depending on the distance of the lens from the image sensor. The distance of the lens from the sensor is set by a precise stepper motor. We looking for the distance at which the scanned image is the sharpest. The appropriate sharpness function should at least meet these criteria [1]:

- *unimodality* – the sharpness function has one distinct extreme,

- *precise* – the highest sharpness is at the extreme of the function,
- *monotonicity* – the sharpness function is mostly monotone in a sufficient distance from the extreme.

There are many suitable sharpness functions. According to [15, 19], we can divide them into functions based on differentials, image convolution, image statistics, autocorrelation, image histogram, the Fourier transform, image entropy and others. All sharpness functions utilize the fact that details in the image are more significant when the image is sharper.

When finding an extreme, it is possible to use function smoothing (e.g. by moving average), if rapid changes (oscillations) occur in the sharpness function [16]. Since the color image is composed of three color components, either the image has to be converted to gray-scale or the sharpness function is evaluated only for one color component [5].

Let us have a picture of $M \times N$ pixels with the intensity values $I(x, y)$, for $x = 0, 1, \dots, M - 1$ and $y = 0, 1, \dots, N - 1$. Let T be properly chosen threshold and k be the size of the difference.

Sharpness functions based on differences

These functions calculate the sharpness measure by using the sum of the differences for neighboring pixel values, either horizontally or vertically, or both [1, 5, 15, 19]. In general, the difference between more than two rows or columns ($k > 1$) may be used. This partially eliminates the sensitivity of these functions to image noise [1].

$$\begin{aligned}
 S_{df,1}(x, y) &= \sum_{x=0}^{M-k-1} \sum_{y=0}^{N-1} |I(x+k, y) - I(x, y)| \text{ or } S_{df,1}(x, y) = \sum_{x=0}^{M-1} \sum_{y=0}^{N-k-1} |I(x, y+k) - I(x, y)|, \\
 S_{df,2}(x, y) &= \sum_{x=0}^{M-k-1} \sum_{y=0}^{N-k-1} (|I(x+k, y) - I(x, y)| + |I(x, y+k) - I(x, y)|), \\
 S_{df,3}(x, y) &= \sum_{x=0}^{M-k-1} \sum_{y=0}^{N-1} (I(x+k, y) - I(x, y))^2 \text{ or } S_{df,3}(x, y) = \sum_{x=0}^{M-1} \sum_{y=0}^{N-k-1} (I(x, y+k) - I(x, y))^2, \\
 S_{df,4}(x, y) &= \sum_{x=0}^{M-k-1} \sum_{y=0}^{N-k-1} ((I(x+k, y) - I(x, y))^2 + (I(x, y+k) - I(x, y))^2),
 \end{aligned}$$

The k value is usually 1 or 2, but it is stated in [1] that a value less than 10 can be used in general.

Sharpness functions based on image convolution

These functions use image filters that emphasize edges in an image when a suitable threshold value of T is chosen [1, 5, 15, 16, 19]. Such filters use numerically calculated partial derivatives by forward difference $\frac{\partial I(x, y)}{\partial x} = I(x+1, y) - I(x, y)$ and $\frac{\partial I(x, y)}{\partial y} = I(x, y+1) - I(x, y)$ or by central difference $\frac{\partial I(x, y)}{\partial x} = \frac{1}{2} (I(x+1, y) - I(x-1, y))$ and $\frac{\partial I(x, y)}{\partial y} = \frac{1}{2} (I(x, y+1) - I(x, y-1))$. Forward differences are used in the Laplace operator $L(x, y) = \nabla^2 I(x, y) = \frac{\partial^2 I(x, y)}{\partial x^2} + \frac{\partial^2 I(x, y)}{\partial y^2}$,

central differences are used in the Sobel filters $G_x(x, y) = \frac{\partial}{\partial x}(g_\sigma * I)(x, y)$ and $G_y(x, y) = \frac{\partial}{\partial y}(g_\sigma * I)(x, y)$. Because these features are very sensitive to image noise, they often use Gaussian function $g_\sigma(x, y) = \frac{1}{2\pi\sigma^2} e^{-\frac{x^2+y^2}{2\sigma^2}}$ for image blurring. The resulting sharpness function is computed by pixels $I'(x, y)$ calculated from the convolution of the $I(x, y)$ with given function $\omega(x, y)$

$$I'(x, y) = (\omega * I)(x, y) = \sum_{r=-1}^1 \sum_{s=-1}^1 \omega(x, y) I(x - r, y - s).$$

When using the Laplace filter, sharpness function is calculated by

$$S_{ic,1}(x, y) = \sum_{x=1}^{M-2} \sum_{y=1}^{N-2} |L(x, y)|, \text{ while } |L(x, y)| > T,$$

If we use the Sobel filters, we get the sharpness function

$$S_{ic,2}(x, y) = \sum_{x=1}^{M-2} \sum_{y=1}^{N-2} (G_x(x, y)^2 + G_y(x, y)^2), \text{ while } \sqrt{G_x(x, y)^2 + G_y(x, y)^2} > T,$$

The Gauss filter is also used in functions that use the Laplace operator

$$S_{ic,3}(x, y) = LoG(x, y) = \nabla^2(g_\sigma * I)(x, y),$$

or use difference of two Gauss filters with standard deviations σ_1 a σ_2

$$S_{ic,4}(x, y) = DoG(x, y) = ((g_{\sigma_1} - g_{\sigma_2}) * I)(x, y).$$

Sharpness functions based on image statistics

These functions typically evaluate the sharpness function using mean absolute error or mean square error [1, 5, 15, 16, 19].

Sharpness functions based on autocorrelation

In this case, the sharpness functions are evaluated by autocorrelation of the image function, which expresses the dependence between adjacent pixels or the dependence of the deviations between adjacent pixels [1, 15, 19].

$$\begin{aligned} S_{ac,1}(x, y) &= \sum_{x=0}^{M-k-1} \sum_{y=0}^{N-1} (I(x+k, y)I(x, y) - \bar{I}^2) \text{ or } S_{ac,1}(x, y) = \sum_{x=0}^{M-1} \sum_{y=0}^{N-k-1} (I(x, y+k)I(x, y) - \bar{I}^2), \\ S_{ac,2}(x, y) &= \sum_{x=0}^{M-k-1} \sum_{y=0}^{N-1} (I(x+k, y) - \bar{I})(I(x, y) - \bar{I}) \text{ or } S_{ac,2}(x, y) = \sum_{x=0}^{M-1} \sum_{y=0}^{N-k-1} (I(x, y+k) - \bar{I})(I(x, y) - \bar{I}), \\ S_{ac,3}(x, y) &= \sum_{x=0}^{M-k-1} \sum_{y=0}^{N-1} I(x+k, y)I(x, y) - \sum_{x=0}^{M-k-l-1} \sum_{y=0}^{N-1} I(x+k+l, y)I(x, y), \end{aligned}$$

or

$$S_{ac,3}(x, y) = \sum_{x=0}^{M-1} \sum_{y=0}^{N-k-1} I(x, y+k)I(x, y) - \sum_{x=0}^{M-1} \sum_{y=0}^{N-k-l-1} I(x, y+k+l)I(x, y).$$

The k (or l) value can be equal to 1 or 2, as in the sharpness function based on differences.

Sharpness functions based on the Fourier transform

The Fourier transform based sharpness functions are computationally intensive but less sensitive to image noise. These functions need to convert the input image to a frequency domain using a discrete Fourier transform (DFT) [1, 5, 13, 19] or using a discrete cosine transform (DCT) [10]. The sharpness functions are calculated by the sum of the transformed values in the frequency range. Higher frequency values are greater in the focused image, but lower in the unfocused image. Similarly, the values at lower frequencies are greater for the unfocused image and smaller for the focused image [13]. When defining sharpness functions, it is often appropriate to use a certain frequency range $\langle T_{low}, T_{high} \rangle$ only [1].

The discrete Fourier transform $F(u, v)$ of the image function $I(x, y)$ is calculated by

$$F(u, v) = \frac{1}{MN} \sum_{x=0}^{M-1} \sum_{y=0}^{N-1} I(x, y) e^{-i2\pi(u\frac{x}{M} + v\frac{y}{N})}.$$

It is derived from the continuous Fourier transform of the image function

$$F(u, v) = \int_{-\infty}^{\infty} \int_{-\infty}^{\infty} I(x, y) e^{-i2\pi(ux+vy)} dx dy.$$

If we use the relation for the exponential form of complex numbers, we can write the DFT using a real and imaginary component

$$\begin{aligned} F(u, v) &= \frac{1}{MN} \sum_{x=0}^{M-1} \sum_{y=0}^{N-1} I(x, y) \cos\left(2\pi\left(u\frac{x}{M} + v\frac{y}{N}\right)\right) + i \frac{1}{MN} \sum_{x=0}^{M-1} \sum_{y=0}^{N-1} -I(x, y) \sin\left(2\pi\left(u\frac{x}{M} + v\frac{y}{N}\right)\right) \\ &= \text{Re}(F(u, v)) + i\text{Im}(F(u, v)). \end{aligned}$$

The magnitude of DFT can be expressed as

$$|F(u, v)| = \sqrt{\text{Re}(F(u, v))^2 + \text{Im}(F(u, v))^2},$$

and the angle (or phase) as

$$\arg(F(u, v)) = \arctan\left(\frac{\text{Im}(F(u, v))}{\text{Re}(F(u, v))}\right).$$

We can now calculate the sharpness function using one of the relations below.

$$S_{ft,1}(x, y) = \sum_{u=0}^{M-1} \sum_{v=0}^{N-1} |F(u, v)|, \text{ for } T_{low} < u + v < T_{high},$$

$$S_{ft,2}(x, y) = \sum_{u=0}^{M-1} \sum_{v=0}^{N-1} ||F(u, v)| \arg(F(u, v))|,$$

$$S_{ft,3}(x, y) = \sum_{u=0}^{M-1} \sum_{v=0}^{N-1} F_{norm}(u, v) \log(F_{norm}(u, v)), \text{ where } F_{norm}(u, v) = \frac{|F(u, v)|}{\sum_{u=0}^{M-1} \sum_{v=0}^{N-1} |F(u, v)|}.$$

For use in photography, the most appropriate functions are sharpness functions based on differences, followed by functions based on the convolution of the image. The worst results are given by functions based on image statistics and image histograms that do not provide sufficient accuracy [15, 19]. Sharpness functions based on the Fourier transformation are robust enough not only for the various surface structure of the scanned object, but also for different light conditions and also for noise in the image [10, 13]. Their accuracy is somewhat worse than for the previous methods [19].

The Cruse scanner in manual focus mode uses a sharpness function based on the Fourier transform function. The scanner has an advanced manual focus interface, which can be seen in Fig. 1. In this interface, it is possible to change the lens distance (Current Position) from the CCD sensor by adjusting the speed of the stepper motor that moves the lens (Lens Speed), or the entire scanning head (Head Speed). To calculate the sharpness function, we chose picture size 41×1 pixels and the green color channel. We set the minimum threshold (Black Threshold) to 0.25 and the maximum threshold (White Threshold) to 0.75. The scanner control algorithm then calculated the sharpness measure (Installation Items – Current) for the current position of the continuously moving lens and displayed the highest value (Installation Items - Max). After verifying the maximum value using the graph of sharpness function (Fig. 2), we set the scanning head and the lens to position (Optimum At :) in which the sharpness function had the highest value.

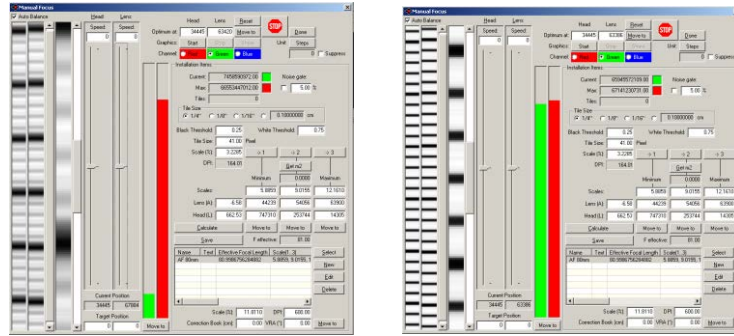


Fig. 1. Cruse Manual Focus Dialog: unfocused picture (left), focused picture (right).

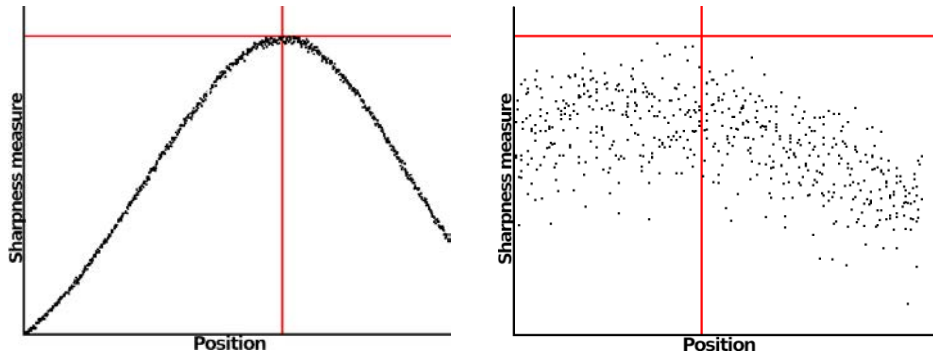


Fig. 2. Graph of sharpness function (left), detail of the graph with noise (right).

The magnified picture of one scanned column of the unfocused image is shown in Fig. 2 on the left and the picture of the focused image in Fig. 2 on the right. Focused image has greater values of the sharpness measure and alternating sharply bounded black and white stripes.

Manual focusing has been verified by scanning multiple objects at multiple resolutions on the improperly calibrated scanner. One of these objects was the black-and-white ruler (Fig. 3) with height $h = 0.0\text{cm}$ scanned at 600 ppi. The $4\times$ magnified view of the image (Fig. 4 left) shows an insufficiently focused image. The scanner allows obtaining a sharp image by setting the artificial (other than the real) height of the object, but at the cost of increased chromatic aberration (Fig. 4 center). Using the $S_{ft,1}(x,y)$ sharpness function, we have achieved a significantly sharper image without chromatic aberration (Fig. 4 on the right) after manual focusing.

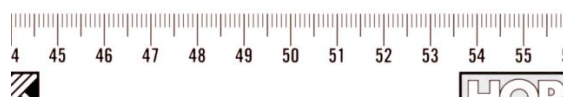


Fig. 3. Picture of scanned black & white ruler.

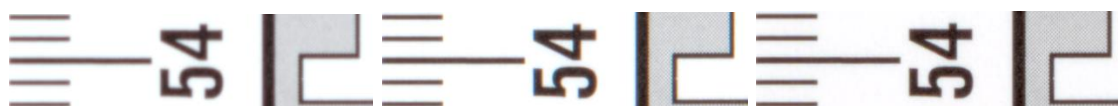


Fig. 4. Unfocused, $h=0.0\text{cm}$ (left); unfocused, $h=1.4\text{cm}$ (center); focused, $h=0.0\text{cm}$ (right).

Thanks to manual focusing, the Cruse Synchron Table scanner allows obtaining a sharp image even if it is badly calibrated or if object height is wrongly estimated. It uses a relatively robust sharpness function based on the Fourier transform. Since there are many sharpness functions in the literature, we have attempted to write a simple list and give mathematical foundation for the most commonly used.

4 Interior of Neologic Synagogue

The Neologic Synagogue in Bratislava was abolished in 1969, when the destruction was photographed by Pavel Breier (Fig. 5). The author agreed with documenting his photocollection by Marek Zimanyi in 2001 and using the data for educational purposes. The exterior model of the lost building was relatively easy to reconstruct. This did not hold for interior, which became the main contribution of a project by Marian Fabian. There were no data available, but fortunately, the original floorplans by B. Milch, dated 1893, were discovered and scanned.



Fig. 5. Original photo by Pavel Breier, photographed by Marek Zimanyi (left). Cruse scans used for exact interior reconstruction (center). Probable light distribution, as seen from the north side of the synagogue [7] (right).

Ten original documents 60×73 cm helped to reconstruct the precise model of the lost building interiors, floor by floor (Fig. 5). The scanning was very slow, three hours. Finally, it remained unclear only, how to enter one part of interior. Marian Fabian discovered this uncertainty in his project [7] in the year 2016. Usually, the hypothetic parts of ancient buildings are modeled as semitransparent. Such a knowledge in metadata can be mentioned. For the same reason the interior is not textured, but for presentation purposes this can be done using pseudodata from similar Maur style synagogues, which survived. The error of the model is about 1 cm.

5 The Art of Scanning Blank Rare Papers

Department of Fine Arts and Education UKF Nitra uses a unique modern equipment and orientation towards the most progressive technologies. Even the top-shelf software Rebelle from the world renowned Slovak company Escape Motions is available for students. The unique **Collection of Rare Handmade Papers (CRHP)** of over 600 items is maintained by Mgr. Ľubomír Zabadal, PhD. These rare papers can be embedded in the digital environment, which assumes highly detailed scanning and appropriate presentation processing. Rebelle was successfully presented at Siggraph 2016 and, it is used by multiple Hollywood studios. It is considered by professionals to be the world's top 3 real-media graphics program and No. 1 in the field of watercolor simulation. For simulation quality, one of the three basic components is a high-quality surface scan that, in conjunction with fluid physics, generates the resulting simulation effect. The Rebelle program has received eight awards [6]. Handmade rare papers essentially affect the result of the painting process, see Fig. 6.



Fig. 6. Scanned empty handmade paper Yucca and the detail of its use with Rebelle software.

The explored set CRHP is a collection of over 600 sheets of papers representing Western European, Central European and East Asian technology for paper making for artistic use. Part of the Western European and Central European tradition is represented by samples of handmade paper using a mold. Selected samples represent the top of the art-historical and art-technological aspect. The East Asian tradition is represented by Japanese, Korean, Chinese and Nepalese paper production. This part of the set is classified according to the method of pumping from the solid form (tamezuki) and the removable form (nagashizuki). Part of the study will be the issue of the aura of the original and the expression of the digital copy. The pilot CRHP set digitization will serve for documentation, Rebelle presentation, and education.

The first scanning experiments resulted in hopeless outcomes. There was no contrast, questionable sharpness and too much light. We had to limit the light intensity using a side mirror light redirection and we halved the integration time. Finally, our searching converged to an

acceptable alternative with mirrored light flow from the left lamp and a half of integration time. The metadata open problem is how to catalogize CRHP in terms of cultural heritage.

6 Comenius University Herbarium

The Department of Botany cultivates a **Herbarium of Comenius University** with an international SLO collection abbreviation. It was established in 1940 and currently includes more than registered 175,000 plant and mushroom items. This collection can be nicknamed The Largest Unpublished Book in Slovakia. The rare items include collections of the first Slovakia's female botanist **Izabela Textorisová** (1866-1949), 4755 items in total, still a valuable source for botanists to this date. She described more than a hundred new plants in the Turiec region. In 1893 she discovered a new species of thistle, later named *Carduus textorisianus* Marg. in her honor [18]. Experimental scanning of hundreds of original SLO documents will be needed to effectively estimate quality and fine-tune batch processing and presentation processes. They will be selected and curated by a renowned herbalist Mgr. Michal Hrabovský, PhD. The digitization outcome should serve for documentation, presentation, and education.

The herbarium item, to be eligible for further scientific studies, must be accompanied by a label or a revision card, if the item was overdestined, plus a color range of base colors and a scale. The label must describe the exact location, the collector's name, the date of collection, the name of the item, or the name of the plant designator if there cooperated an assistant collector. Concerning the use of herbarium items, there is a wide range of cultural heritage conservation, through the monitoring of the dynamics of the endangered or invasive plants in the long run, after morphometric studies for taxa. It would be desirable to disseminate the herbarium value and, eventually, improve its uncertainties in color or completeness.

7 Conclusion and Future Work

Our main contributions can be seen in a survey of tens of evaluation functions, experiments with manual focusing, and reconstruction of missing interior of an important memorial. Moreover, we have found two unique sets of primary data (originals) SLO and CRHP containing hand-made originals, typically in the A3 format. These collections have a world-class meaning in their areas. We prepare both mid-scale CRHP and large-scale SLO documentation. For both prominent data sets, there is no documentation in presented accuracy class. It can be expected that it will be possible for the Herbarium ask the new scientific questions or reverse aging of grayfaded parts with colors of fresh plants. For the CRHP collection, we expect to use the scans in the Rebelle software tool by Escape Motions. The reported sharpness experiments we will complement with color precision verifications.

We intend to enhance the quality of research and development of innovation for the intelligent specialization of the new hi-tech scanning facility at FMFI UK. The Cruse scanning allows for a highly detailed presentation. Last but not least, we will share the data and experience within the new Data Science study program. For teaching the standard scanning, we started to create two prominent datasets, video tutorials [14] and a textbook for our students.

Acknowledgement

The Cruse scanner was supported by Comeniana grant No. ITMS 26240220077 (OPVaV-2011/4.2/07-SORO) and it moved from EDICO SK to FMFI UK. We would like to thank the owners of originals, Múzeum židovskej kultúry in Bratislava, MUDr. P. Breier, Dr. M. Zimányi, and EDICO SK for long-term valuable cooperation and support of student projects. This work has been supported by the project KEGA 060UK-4/2018.

References

- [1] BATTEN, C. F. (2000). Autofocusing and astigmatism correction in the scanning electron microscope. *Mphil thesis, University of Cambridge*.
- [2] BOHUMELOVÁ, M. ed. 2015. *Rituál múzea v digitálnom veku*. [online] https://issuu.com/sng.sk/docs/ritualmuzea_online/47. (November 15, 2018.)
- [3] Cruse software CSx 3.9. Manual. 2018. CRUSE Spezialmaschinen GmbH. Gimmersdorfer Str. 76. 53343 Wachtberg, Germany.
- [4] CHAMBERS, M. 2018. Pictureelement, *About Our Scans*. [online]. <http://www.pictureelement.com/aboutcruse.php>. (November 15, 2018.)
- [5] CHERN, N. N. K., NEOW, P. A., & ANG, M. H. (2001). Practical issues in pixel-based autofocusing for machine vision. In *Robotics and Automation, 2001. Proceedings 2001 ICRA. IEEE International Conference on* (Vol. 3, pp. 2791-2796). IEEE.
- [6] Escape Motions. [online] <https://www.escapemotions.com/products/rebelle/index.php>. (November 15, 2018.)
- [7] FABIAN, M. 2016. *Virtualizácia bratislavskej synagógy*. Bc Thesis. UK Bratislava.
- [8] FERKO, A. et al. 2011. Virtuálne mestské múzeum. Pp 30-51 In MAJCHROVIČOVÁ, V., ŠULLOVÁ, Z. eds. 2011. *Informačno-komunikačné technológie, využitie v prezentačnej činnosti múzeí*. Banská Štiavnica: ZMS 2011.
- [9] HALUŠKA, J. *The Mathematical Theory of Tone Systems*. NY: Marcel Dekker 2004.
- [10] JEON, J. et al. (2011). Robust focus measure for unsupervised auto-focusing based on optimum discrete cosine transform coefficients. *IEEE Trans. on Consumer Electronics*, 57(1).
- [11] JURKOVIČ, J. 2018. Digitálne Múzeum. [Online]. (November 15, 2018.) <http://www.muzeumsnp.sk/digitalizacia/projekt-digitalne-muzeum/co-je-digitalne-muzeum/>.
- [12] KALUŽNÍKOVÁ, D. 2012. *Definovanie úlohy múzea v súčasnej spoločnosti*. Bratislava: SNM 2012.
- [13] KRISTAN, M., & PERNUS, F. (2004). Entropy based measure of camera focus. In *Proc. of the thirteenth Electrotechnical and Computer Science Conference ERK* (p. 179).
- [14] LÚČAN, Ľ. 2018. *Cruse Scanning Videotutorial*. Bratislava: FMFI UK 2018.
- [15] MIR, H., XU, P., & VAN BEEK, P. (2014, March). An extensive empirical evaluation of focus measures for digital photography. In *Digital Photography X* (Vol. 9023, p. 90230I). International Society for Optics and Photonics.
- [16] PECH-PACHECO, J. L. et al. (2000). Diatom autofocusing in brightfield microscopy: a comparative study. In *Pattern Recognition, 2000. Proceedings. 15th International Conference on* (Vol. 3, pp. 314-317). IEEE.
- [17] Project Comeniana Showreel. [online] <https://www.youtube.com/watch?v=p7l9iIK88r8>. (November 15, 2018.)
- [18] VOZÁROVÁ, M. – ŠÍPOŠOVÁ, H. 2011. *Osobnosti botaniky na Slovensku*. ISBN:978-80-2241-136-3. Bratislava: Veda 2011.

- [19] YAO, Y., ABIDI, B., DOGGAZ, N., & ABIDI, M. (2006, May). Evaluation of sharpness measures and search algorithms for the auto focusing of high-magnification images. In *Visual Information Processing XV* (Vol. 6246, p. 62460G). Int. Society for Optics and Photonics.

Current address

Bátorová Martina, RNDr., PhD.

Faculty of Mathematics, Physics and Informatics, Comenius University in Bratislava
Mlynská dolina, 842 48 Bratislava, Slovak republic
E-mail: batorova@fmph.uniba.sk

Bohdal Robert, RNDr., PhD.

Faculty of Mathematics, Physics and Informatics, Comenius University in Bratislava
Mlynská dolina, 842 48 Bratislava, Slovak republic
E-mail: bohdal@fmph.uniba.sk

Fabián Marián, Bc.

Faculty of Mathematics, Physics and Informatics, Comenius University in Bratislava
Mlynská dolina, 842 48 Bratislava, Slovak republic
E-mail: fabian.marian@gmail.com

Ferko Andrej, doc. RNDr.

Faculty of Mathematics, Physics and Informatics, Comenius University in Bratislava
Mlynská dolina, 842 48 Bratislava, Slovak republic
E-mail: ferko@fmph.uniba.sk

Lúčan Ľubomír, prom. fyz., CSc.

Faculty of Mathematics, Physics and Informatics, Comenius University in Bratislava
Mlynská dolina, 842 48 Bratislava, Slovak republic
E-mail: lucan@fmph.uniba.sk

Hrabovský Michal, Mgr., PhD.

Faculty of Natural Sciences, Comenius University in Bratislava
Department of Botany, Herbarium
Révová 39, 811 02 Bratislava 1,
E-mail: michal.hrabovsky@uniba.sk

Zabadal Ľubomír, Mgr., PhD.

Pedagogická fakulta UKF
Dražovská cesta 4, 949 74 Nitra, Slovak republic
E-mail: zabadalkega@gmail.com